

1 **Nintedanib ameliorates experimental pulmonary arterial hypertension via**
2 **inhibition of endothelial mesenchymal transition and smooth muscle cell proliferation**

3
4
5 Takeo Tsutsumi¹, Tetsutaro Nagaoka¹, Takashi Yoshida¹, Lei Wang¹,
6 Sachiko Kuriyama¹, Yoshifumi Suzuki¹, Yuichi Nagata¹,
7 Norihiro Harada¹, Yuzo Kodama¹, Fumiyuki Takahashi¹, Yoshiteru Morio²,
8 and Kazuhisa Takahashi¹.

9
10 ¹ Department of Respiratory Medicine, Juntendo University Faculty of Medicine & Graduate
11 School of Medicine, 3-1-3 Hongo Bunkyo-ku, Tokyo 113-8431, Japan.

12 ² Department of Respiratory Medicine, National Hospital Organization Tokyo National
13 Hospital, 3-1-1 Takeoka Kiyose-shi, Tokyo 204-8585, Japan.

14
15 **Short title:**

16 Nintedanib for experimental pulmonary arterial hypertension

17
18 **Corresponding Author:**

19 Tetsutaro Nagaoka MD PhD

20 Department of Respiratory Medicine, Juntendo University Graduate School of Medicine
21 3-1-3 Hongo Bunkyo-ku, Tokyo 113-8431, Japan.

22 Tel: +81-3-5802-1063

23 Fax: +81-3-5802-1617

24 E-mail: jnagaoka@juntendo.ac.jp

25
26 **Author contributions:**

27 T.T contributed whole of experiment. T.N supervised whole of this study. T.Y, L.W and S.K
28 assisted in molecular biological experiment. Y.S and Y.N assisted in animal experiment.
29 N.H, Y.K, F.T, Y.M, and K.T assisted in planning of this study.

30

31

32 **Abstract**

33 Neointimal lesion and medial wall thickness of pulmonary arteries (PAs) are common
34 pathological findings in pulmonary arterial hypertension (PAH). Platelet-derived growth
35 factor (PDGF) and fibroblast growth factor (FGF) signaling contribute to intimal and medial
36 vascular remodeling in PAH. Nintedanib is a tyrosine kinase inhibitor whose targets include
37 PDGF and FGF receptors. Although the beneficial effects of nintedanib were demonstrated
38 for human idiopathic pulmonary fibrosis, its efficacy for PAH is still unclear. Thus, we
39 hypothesized that nintedanib is a novel treatment for PAH to inhibit the progression of
40 vascular remodeling in PAs. The inhibitory effects of nintedanib were evaluated both in
41 endothelial mesenchymal transition (EndMT)-induced human pulmonary microvascular
42 endothelial cells (HPMVECs) and human pulmonary arterial smooth muscle cells
43 (HPASMCs) stimulated by growth factors. We also tested the effect of chronic nintedanib
44 administration on a PAH rat model induced by Sugen5416 (a VEGF receptor inhibitor)
45 combined with chronic hypoxia. Nintedanib was administered from weeks 3 to 5 after
46 Sugen5416 injection, and pulmonary hemodynamics and PAs pathology were evaluated.
47 Nintedanib attenuated the expression of mesenchymal markers in EndMT-induced
48 HPMVECs and HPASMCs proliferation. Phosphorylation of PDGF and FGF receptors was
49 augmented both in both intimal and medial lesions of PAs. Nintedanib blocked these

50 phosphorylation, improved hemodynamics and reduced vascular remodeling involving
51 neointimal lesions and medial wall thickening in PAs. Additionally, expressions Twist1,
52 transcription factors associated with EndMT, in lung tissue was significantly reduced by
53 nintedanib. These results suggest that nintedanib may be a novel treatment for PAH with
54 anti-vascular remodeling effects.

55

56 Word count: 247

57

58 **Introduction**

59 The pathogenesis of pulmonary arterial hypertension (PAH) involves abnormal
60 vasoconstriction and vascular remodeling in pulmonary arteries (PAs). Various stimuli,
61 including hemodynamic stress, hypoxia, and inflammation, alter endothelial cell functions
62 and cause an imbalance in endothelial cell-derived vasoconstrictive and vasodilative factors
63 (1). Endothelin-1, prostacyclin, and nitric oxide are major regulators of vascular tone, and
64 several types of vasodilators for PAH have been developed that target these signaling
65 pathways. Although the prognosis of PAH has been remarkably improved by these
66 vasodilators (2, 3), there is still no drug that targets vascular remodeling in PAH.

67 Pulmonary arterial remodeling plays an essential role in the progression of PAH, especially
68 in the late phase of disease. Previous studies have suggested that platelet derived growth
69 factor (PDGF) and fibroblast growth factor (FGF) signaling contribute to vascular cell
70 proliferation, migration, differentiation, and apoptosis (4). Expressions of PDGF-A, PDGF-B,
71 PDGF receptor- α , and PDGF receptor- β are increased in the PAs of PAH patients
72 compared with those of healthy patients (5). Previous reports have also demonstrated
73 elevated basic FGF concentration in the plasma from PAH patients (6). FGF2 signaling
74 mediated by FGF receptor 1 (FGFR1) promotes proliferation of vascular endothelial cells (7)
75 and smooth muscle cells (8) in human PAH. Additionally, endothelial mesenchymal

76 transition (EndMT) has been suggested to contribute to the progression of occlusive
77 neointimal lesions in PAs, which is a characteristic vascular abnormality in PAH (9, 10).
78 Vascular endothelial cells acquire a mesenchymal phenotype following exposure to several
79 cytokines and growth factors, including transforming growth factor β (TGF- β), PDGF, and
80 FGF which are induced by shear stress, hypoxia, and inflammation (10). EndMT-modified
81 endothelial cells acquire additional characteristics of mesenchymal cells, and recent reports
82 have indicated a critical role of EndMT in the development of PAH-specific neointimal
83 lesions in PAs (11-13). Although both medial wall thickness and neointimal lesions in PAs
84 are common pathological findings in PAH, a greater contribution of neointimal lesions in the
85 elevation of pulmonary arterial pressure was reported in experimental PAH (14), suggesting
86 an important involvement of EndMT.

87 Nintedanib is a triple tyrosine kinase inhibitor (TKI) of PDGF, FGF, and vascular endothelial
88 growth factor (VEGF) receptors (15). A recent phase III clinical study showed that nintedanib
89 prevented both the progression of restrictive pulmonary impairment and the acute
90 exacerbation of idiopathic pulmonary fibrosis (IPF), with good tolerability (16). Thus,
91 nintedanib was approved globally for the treatment of IPF. However, the efficacy of
92 nintedanib to treat PAH by inhibiting PDGF and FGF signaling is still uncertain. Based on
93 this background information, we hypothesized that nintedanib is a novel and beneficial

94 treatment for PAH by targeting vascular remodeling including neointimal lesion and medial
95 wall thickening in PAs.

96

97 **Materials and Methods**

98 Primary human pulmonary microvascular endothelial cells (HPMVECs; product code.
99 CC-2527, lot no. 547317, 560121, and 621712) and primary human pulmonary arterial
100 smooth muscle cells (HPASMCs; product code. CC-2581, lot no. 029837, 407340, and
101 559495) were obtained from Lonza (Basel, Switzerland). All experimental and surgical
102 procedures were approved by the Institutional Committee for the Use and Care of
103 Laboratory Animals in Juntendo University (Tokyo, Japan), in accordance with the U.S.
104 National Institutes of Health Guide for the Care and Use of Laboratory Animals.

105 ***EndMT of HPMVECs***

106 HPMVECs were cultured in Microvascular Endothelial Cell Growth Medium-2
107 (EGMTM-2MV, Lonza). TGF- β 2 (2.5 ng/mL), tumor necrosis factor (TNF)- α (2 ng/mL), and
108 interleukin (IL)-1 β (4 ng/mL) were used for the induction of EndMT as previously described
109 (17). The cytokines were added to the medium with or without a 3-h preincubation with
110 nintedanib (1 μ M). This concentration of nintedanib had been confirmed to have maximum
111 inhibitory effects in preliminary experiments. The expressions of von Willebrand factor

112 (vWF) and CD31 proteins, which are endothelial markers, as well as fibronectin and
113 collagen 1 proteins, which are mesenchymal markers, were analyzed at 48 h after
114 stimulation by western blotting to confirm EndMT of the HPMVECs.

115 ***Proliferation assay of HPASMCs***

116 HPASMCs were cultured in Smooth Muscle Growth Medium-2 (SmGM™-2, Lonza). The
117 proliferation of HPASMCs was evaluated using both the Cell Counting Kit-8 (CCK-8) and
118 Bromodeoxyuridine (BrdU) ELISA kit as previously described, respectively (18, 19).
119 HPASMCs were treated with multiple growth factors, specifically 5% fetal calf serum,
120 PDGF-BB (30 ng/mL), FGF2 (2 ng/mL), epidermal growth factor (EGF) (0.5 ng/mL), and
121 insulin-like growth factor-1 (IGF-1) (0.5 µg/mL) with or without imatinib (3 µM) or nintedanib
122 (0.3 µM). The viability of HPASMCs was evaluated time-dependently after stimulation. In
123 advance of this assay, we examined the concentration-dependent inhibitory effects of
124 nintedanib and imatinib, the latter of which is another TKI for PDGF signaling, on the
125 proliferation of HPASMCs induced by PDGF-BB. Based on these preliminary results, we
126 selected 0.3 µM and 3 µM of nintedanib and imatinib, respectively, as concentrations that
127 produced maximum inhibitory effects. LDH assay was also performed to assess the cell
128 toxicity of nintedanib and imatinib as previously described (20). Value of LDH in the medium
129 with nintedanib and imatinib were normalized by that in the control medium without TKI.

130 The protein expression of extracellular signal-regulated kinase (ERK)1/2 and AKT with or
131 without phosphorylation, which are downstream effectors of PDGF and FGF signaling, was
132 also evaluated by western blotting at 2 h after stimulation of the HPASMCs.

133 ***Preparation of pulmonary hypertensive rats***

134 The PAH rat model was established using Sugen 5416 (VEGF receptor-1,-2 inhibitor) and
135 chronic hypoxic exposure as previously described (14, 21). Briefly, adult male Sprague
136 Dawley rats (150 – 180 g) were injected with Sugen 5416 (20 mg/kg; Cayman Chemical Co,
137 MI) subcutaneously and exposed to hypobaric hypoxia (360 mmHg, 10% O₂) for 3 weeks.
138 After returning to normoxic conditions (760 mmHg, 21% O₂), the rats were analyzed
139 immediately [SuHx(3W) group] or were chronically treated with either vehicle (0.5%
140 hydroxyethylcellulose) [SuHx(5W) group] or nintedanib [50 mg/kg/day, SuHx(5W) + Nin
141 group] by oral gavage for 2 weeks. The dose of nintedanib was determined based on
142 previously published experiments (15). Control rats received a single vehicle injection and
143 were exposed to normoxic conditions for 5 weeks, with vehicle or nintedanib (50 mg/kg/day)
144 gavage from 3 to 5 weeks [Nx(5W)] and [Nx(5W) + Nin] groups, respectively. Hemodynamic
145 measurements were performed at 3 or 5 weeks after vehicle or Sugen 5416 injection.

146 ***Pulmonary hemodynamic measurements***

147 Pulmonary hemodynamic measurements by right heart catheterization were performed as
148 previously described (22). Briefly, all rats were anesthetized with pentobarbital sodium (30
149 mg/kg intraperitoneal). A polyvinyl catheter was inserted into the right ventricle (RV) via the
150 right jugular vein for the measurement of RV systolic pressure (RVSP) with the PowerLab
151 data acquisition system (AD Instruments, CO). Systemic systolic arterial pressure (SAP)
152 and heart rate (HR) were continuously monitored, and rats with an HR of consistently less
153 than 300 beats/min were excluded. After the hemodynamic measurements, all rats were
154 euthanized by an overdose of pentobarbital sodium, and their hearts and lungs were
155 collected for RV / left ventricle (LV) + septum weight ratio (RV/LV+S) measurements to
156 show RV hypertrophy and for histological evaluations. The right lungs were stored for
157 protein measurement, and the left lungs were inflated with 10% buffered formalin at a
158 constant pressure of 20 cm H₂O for histological analyses. Fixation was allowed to proceed
159 overnight.

160 ***Morphological analysis of PAs***

161 The inflated and fixed left lungs were embedded in paraffin. All sections were cut at 5- μ m
162 thickness and were stained with elastic Van Gieson stain. A quantitative analysis of PA
163 luminal obstruction was performed as described previously with minor modifications (14).
164 We counted between 100 and 200 small PAs [outer diameter (OD) < 200 μ m] per whole left

165 lobe at $\times 400$ magnification using an image analysis system (KS400; Carl Zeiss Imaging
166 Solutions, Germany) in a blind manner. The medial-wall thickness was measured for the
167 arteries with an OD between 50 and 200 μm . The distance between the internal and
168 external elastic laminae was expressed as the medial thickness/OD. Vessels with an OD $<$
169 50 μm were used for the assessment of occlusive neointimal lesions and were scored as
170 follows: no evidence of occlusive neointimal formation (grade 0), partial luminal occlusion (\leq
171 50%; grade 1), and severe luminal occlusion ($>$ 50%; grade 2).

172 ***Immunohistochemistry of PAs***

173 After deparaffinization with xylene, rehydration, and antigen retrieval by heating in citrate
174 buffer (pH 6), immunohistochemistry was performed with an anti-FGFR1 (phospho Y654)
175 antibody (ab59194, Abcam, Cambridge, UK), anti-PDGF receptor- β (phospho Y1020)
176 antibody (ab16868, Abcam, Cambridge, UK). The signals were detected using
177 VECTASTAIN[®] elite ABC rabbit, mouse and goat IgG kits (#PK-6101, 6102, 6105, Vector
178 Laboratories, CA). In each whole left lobe, 100 arteries across serial sections were
179 examined to evaluate the expression of each receptor.

180 ***Expression of Twist1 in rat lung tissues***

181 The expression of Twist1 protein, which is an EndMT-related transcription factor (11), was
182 evaluated by western blotting in lung tissues from Nx(5W), SuHx(5W), and SuHx(5W) + Nin

183 groups to assess the contribution of EndMT in the vascular remodeling of PAs in rat PAH
184 and to assess the anti-EndMT effect of nintedanib.

185 ***Western blotting analysis***

186 HPASMCs, HPMVECs, and lung tissues were lysed in radioimmunoprecipitation assay
187 (RIPA) buffer containing protease and phosphatase inhibitors, and the lysates were
188 subjected to western blotting, as described previously (23). Transferred membranes were
189 allowed to react with anti-vWF polyclonal antibody (1:1,000; sc14014, Santa Cruz
190 Biotechnology), anti-CD31 monoclonal antibody (1:2,000; bba7, R&D Systems, MN),
191 anti-fibronectin monoclonal antibody (1:2,000; sc59826, Santa Cruz Biotechnology),
192 anti-Collagen 1 polyclonal antibody (1:1,000; ab34710, Abcam), anti-p44/42 MAPK (Erk1/2)
193 Antibody (1:2,000; #9102, Cell Signaling Technology), anti-Phospho-p44/42 MAPK (Erk1/2)
194 (Thr202/Tyr204) Antibody (1:2,000; #9101, Cell Signaling Technology), anti-AKT polyclonal
195 antibody (1:2,000; #9272, Cell Signaling Technology), anti-phospho-AKT (Ser473)
196 polyclonal antibody (1:2,000; #9271, Cell Signaling Technology), anti-Twist1 polyclonal
197 antibody (1:1000; ab50581, Abcam), or anti- β -actin monoclonal antibody (1:10,000; A5441,
198 Sigma, MO). Western blot signals were acquired using a Fuji ImageQuant™ LAS-4000
199 fluorescence imager and quantified using the Multi Gauge image analysis software (Fujifilm
200 Corporation, Tokyo, Japan). The densitometric signal of each protein was normalized to that

201 of β -actin.

202 ***Statistical analysis***

203 Data are presented as means \pm SE. Statistical analysis was performed using one-way
204 ANOVA (Prism 6; GraphPad Software, La Jolla, CA, USA). Differences were considered
205 significant at $P < 0.05$.

206

207 **Results**

208 ***Inhibitory effect of nintedanib on EndMT of HPMVECs***

209 We confirmed decreased expression of vWF and CD31 proteins and increased expression
210 of fibronectin and collagen 1 proteins by western blotting. Nintedanib attenuated the
211 upregulation of mesenchymal markers in the stimulated HPMVECs, but did not prevent the
212 downregulation of endothelial markers (Figure 1A, B). After stimulation with TGF- β 2, TNF- α ,
213 and IL-1 β , the morphology of HPMVECs changed from a cobblestone to spindle-shaped
214 morphology, and nintedanib tended to prevent its change. (Figure 1C).

215 ***Inhibitory effect of nintedanib on proliferation of HPASMCs***

216 The proliferation of HPASMCs induced by multiple growth factors (PDGF-BB, FGF2, EGF,
217 and IGF) was significantly greater than that without stimulation in CCK-8 and BrdU assays,
218 and nintedanib significantly inhibited this proliferation at 24 and 48 h after stimulation.

219 Moreover, the inhibitory effect of nintedanib was significantly greater than that of imatinib at
220 48 h after stimulation in CCK-8 assay (Figure 2A, 2B). Values of LDH in the medium after
221 treatment with imatinib and nintedanib were similar between all groups (Figure 2C). The
222 phosphorylation of ERK1/2 and AKT was increased in the HPASMCs stimulated with
223 multiple growth factors, and nintedanib remarkably prevented these phosphorylations. This
224 preventive effect of nintedanib was significantly greater than that of imatinib on the
225 phosphorylated AKT (Figure 2D).

226 ***Chronic treatment with nintedanib in PAH rats***

227 The rats were divided into 5 groups as follows: 5-week normoxia + vehicle group [Nx(5W)],
228 5-week normoxia + nintedanib group [Nx(5W) + Nin], Sugen 5416 + hypoxia + vehicle
229 group [SuHx(3W) and SuHx(5W)], and Sugen 5416 + hypoxia + nintedanib group
230 [SuHx(5W) + Nin] (Figure 3A). Three weeks after Sugen 5416 injection and hypoxic
231 exposure, the RVSP and RV/LV+S were already higher in the SuHx(3W) group (81.3 ± 2.7
232 mmHg and 0.688 ± 0.034 , respectively) than in the Nx(5W) group (22.4 ± 1.1 mmHg and
233 0.296 ± 0.014 , respectively). After 2 weeks of treatment with nintedanib [SuHx(5W) + Nin],
234 the RVSP and RV/LV+S were significantly reduced (50.4 ± 7.2 mmHg and 0.546 ± 0.029 ,
235 respectively) compared with those of the SuHx(5W) group (81.8 ± 6.6 mmHg and $0.728 \pm$
236 0.023 , respectively). Treatment with nintedanib under normoxic condition [Nx(5W) + Nin]

237 caused no effect on pulmonary hemodynamics (Figure 3B). Chronic treatment with
238 nintedanib also did not affect the systemic SAP, HR, or body weight (Figure 3C). The values
239 of RVSP and RV/LV+S in the SuHx(5W) rats are consistent with those of a previous study
240 (14).

241 The medial wall thickness of PAs (50 to 200 μm OD) in the [SuHx(5W)+Nin] group was
242 significantly reduced compared to that in the SuHx(3W) and SuHx(5W) groups. The grade 1
243 and grade 2 neointimal occlusive lesions in the small PAs ($< 50 \mu\text{m}$ OD) were also
244 significantly lower in [SuHx(5W) + Nin] than in SuHx(3W) and in SuHx(5W). Although the
245 medial wall thickening and grade 1 neointimal occlusive lesions were reversed by treatment
246 with nintedanib compared with the SuHx(3W) values, nintedanib treatment lessened, but did
247 not reverse, the development of grade 2 neointimal occlusive lesions (Figure 4A, B). Both
248 medial wall thickness and neointimal lesions with the severe PH group tended to be
249 progressive compared to those of the less severe PH group.

250 ***Phosphorylation of FGF and PDGF receptors in PAs***

251 The expression of phosphorylated FGFR1 and PDGF receptor- β were significantly
252 increased not only in PAs with medial wall thickening (OD 50–200 μm), but also in PAs with
253 occlusive neointimal lesions (OD $< 50 \mu\text{m}$), in contrast to the low levels in the PAs of Nx(5W)
254 lungs. The phosphorylation of FGFR1 and PDGF receptor- β in PAs was significantly

255 decreased by 2-week treatment with nintedanib [SuHx(5W) + Nin] (Figure 5A, B).

256 ***Expression of Twist1 in rat lung tissue***

257 The expression of Twist1 protein by western blotting was significantly augmented in lung
258 tissue from SuHx(5W) rats compared with that from Nx(5W) rats, and nintedanib remarkably
259 reduced this augmented expression (Figure 6).

260

261 **Discussion**

262 This report assessed the beneficial effect of nintedanib for PAH both *in vitro* and *in vivo*.
263 Nintedanib attenuated the progression of EndMT in HPMVECs and inhibited the
264 proliferation of HPASMCs *in vitro*. In addition, we demonstrated that phosphorylated PDGF
265 and FGF receptors were increased in vascular occlusive neointimal lesions and the
266 thickening medial wall in PAH rats. Two-week treatment of PAH rats with nintedanib
267 significantly ameliorated pulmonary hemodynamics accompanied with improved vascular
268 remodeling of PAs.

269 ***Mechanism of pulmonary arterial remodeling in PAH***

270 Medial wall thickening and occlusive neointimal lesion of PAs are common pathological
271 findings in PAH. In the remodeling process of PAs in PAH, medial wall thickening driven by
272 proliferation and hypertrophy of smooth muscle cells occurs early in disease progression.

273 Moreover, the contribution of functional changes in smooth muscle cells of different
274 phenotypes occurs particularly in the establish phase (24). On the other hand, a greater
275 contribution of neointimal lesions than of medial wall thickness in the development of PAH
276 was shown in an experimental model (14), and the role of EndMT in the progression of
277 neointimal lesions has been recently suggested (10-13).

278 The essential role of EndMT in the pathogenesis of various cardiovascular diseases and
279 PAH has been recently demonstrated (25). Occlusive neointimal lesions in small PAs,
280 including plexiform lesions, are characteristic in PAH, and the proliferative cells that
281 comprise these PAH-specific neointimal lesions have both endothelial and mesenchymal
282 phenotypes (9, 11). Inducers, such as a hemodynamic stress, mechanical injury, hypoxia,
283 and inflammation, upregulate several growth factors and cytokines, including PDGF, FGF,
284 and TGF- β , which play important roles in the progression of EndMT (26, 27). Endothelial
285 cells lose their intercellular adhesion after exposure to these stimuli, and subsequently
286 change from a cobblestone to spindle-shaped morphology. EndMT-induced endothelial
287 cells express both endothelial and mesenchymal markers, and acquire further capacity to
288 proliferate, migrate, and avoid apoptosis (10). In a PAH model, both endothelial and
289 mesenchymal markers were seen by immunohistochemistry in neointimal lesions of small
290 PAs (12). Recent reports also have shown that green fluorescent protein (GFP)-labeled

291 endothelial cells in mice were transformed by Sugden 5416 injection and chronic hypoxic
292 exposure to a mesenchymal phenotype with high proliferative and migratory abilities (13). In
293 human PAH, Ranchoux *et al.* demonstrated by electron microscopy that caveolae, which
294 are characteristic of vascular endothelial cells, and dense bodies, which are dominant in
295 vascular smooth muscle cells, were present in the same cells comprising occlusive
296 neointimal lesions. Moreover, the expression of Twist1, a transcription factor associated with
297 EndMT, was higher in human PAH lung than in normal human lung (11). These data
298 indicate a critical contribution of EndMT in the progression of neointimal lesions in PAH.

299 ***Tyrosine kinase inhibitors for PAH***

300 Imatinib is a TKI for Bcr-Abl, c-Kit, c-Abl, and PDGF receptor signaling, and has been used
301 for the treatment of chronic myelogenous leukemia and gastrointestinal stromal tumors (28).
302 Imatinib was also expected to be a novel anti-vascular treatment for PAH due to its inhibitory
303 effect on PDGF receptor. Imatinib was shown to inhibit the proliferation of HPASMCs from
304 PAs in human PAH (29), and long-term treatment with imatinib prevented the development
305 of chronic hypoxia- and monocrotaline-induced pulmonary hypertension in rats (30, 31) .
306 Furthermore, imatinib combined with various vasodilators significantly improved 6-minute
307 walking distance and pulmonary vascular resistance in human patients, and a phase III
308 clinical study of imatinib for PAH was implemented (32). However, imatinib did not receive

309 final approval for PAH because of its serious adverse effects. Dasatinib, a TKI for Bcr-Abl,
310 c-kit, Src family and PDGF receptor signaling, has been used also to treat chronic
311 myelogenous leukemia. Importantly, dasatinib-induced pulmonary hypertension has been
312 previously reported, suggesting specific toxicity of dasatinib on pulmonary vessels (33, 34).

313 Nintedanib is a TKI for PDGF, FGF, and VEGF receptors. FGFR1, 2, and 3; PDGF
314 receptor- α and - β ; and VEGF receptor-1, -2, and -3 are receptors that are targeted by
315 nintedanib (35). Nintedanib was originally developed for the treatment of malignancies as an
316 agent to inhibit angiogenesis, cell proliferation, and migration (36). Nintedanib also reduced
317 the mRNA and protein expression of extracellular matrix components in fibroblasts from
318 human IPF (37), indicating the ability of nintedanib to treat IPF. Additionally, a recent phase
319 III clinical study for human IPF showed beneficial effects of nintedanib in improving forced
320 vital capacity and reducing the incidence of acute exacerbations. Diarrhea and liver
321 dysfunction are major adverse effects of nintedanib, but these events were generally well
322 tolerated (16). Hence, nintedanib has been approved globally for the treatment of IPF. In
323 contrast to dasatinib, the results from the phase III study and postmarketing surveillance
324 revealed no evidence to warrant elevating the risk of pulmonary hypertension by nintedanib.

325 Based on this background, we hypothesized that nintedanib was a novel and tolerable
326 treatment for PAH because of its anti-vascular remodeling via inhibition of PDGF and FGF

327 signaling.

328 ***Effect of nintedanib in vitro***

329 In this study, nintedanib significantly prevented the increased expression of mesenchymal
330 markers in EndMT-induced HPMVECs. A recent report showed that nintedanib reduced
331 TGF- β signaling via inhibition of SMAD3 and p38 MAPK pathways (37). TGF- β signaling is
332 considered a major regulator of EndMT, suggesting that the inhibition of TGF- β signaling is
333 one of the mechanisms of the anti-EndMT effect by nintedanib. Moreover, previous reports
334 showed that PDGF and FGF enhanced signaling of p38/AKT and PI3K/AKT pathways.
335 Increased p38/PI3K/AKT signaling affected the expression of endothelial markers involving
336 vWF and CD31 via transcription factors involving Twist1 (25). These data suggest that
337 nintedanib can also regulate EndMT via inhibition of PDGF/FGF receptor tyrosine kinase
338 activity in addition to TGF- β signaling. On the other hand, the reduced expression of
339 endothelial markers was not restored after treatment with nintedanib. HPMVECs were
340 pretreated with nintedanib before induction of EndMT in this study. Blockade of VEGF
341 signaling by nintedanib may disrupt the maintenance of endothelial cell characteristics,
342 because VEGF signaling generally plays an endothelial protective role (38).

343 In HPASMCs, nintedanib also significantly prevented the proliferation induced by multiple
344 growth factors, and the inhibitory effect of nintedanib was significantly greater than that of

345 imatinib after co-stimulation with multiple growth factors. The LDH assay showed no
346 difference even after treatment with nintedanib, suggesting no toxicity of nintedanib for
347 HPASMCs. ERK1/2 and AKT, which are downstream effectors of PDGF and FGF signaling,
348 play roles in the regulation of vascular smooth muscle cell proliferation and apoptosis.
349 Nintedanib also remarkably reduced the phosphorylation of ERK1/2 and AKT after
350 co-stimulation, and this inhibitory effect of nintedanib was greater than that of imatinib.
351 These *in vitro* results suggest a beneficial, anti-remodeling effect of nintedanib in the intima
352 and media of PAs in PAH.

353 ***Effect of nintedanib in vivo***

354 Classical animal models of pulmonary hypertension that are induced by chronic hypoxic
355 exposure and monocrotaline have no neointimal lesions in the small PAs. Hence, these
356 models were considered inappropriate for the study of PAH. In the present study, we used
357 SuHx-PAH rats, which have neointimal lesions similar to those in human PAH (39), to
358 evaluate the effect of nintedanib. Toba *et al.* provided a detailed evaluation of the time
359 course progression of vascular remodeling in the SuHx-PAH rat (14). They observed
360 thickened medial walls and neointimal lesions in PAs from 3 to 5 weeks, whereas fibrotic
361 vasculopathy involving plexiform lesions progressed 8 weeks following injection of Sugen
362 5416. Although the medial wall thickness decreased to a normal range during the late phase

363 of PAH even with an elevated RVSP, the increased density of severely occlusive PAs was
364 obviously correlated with RVSP elevation. Thus, the authors concluded that the contribution
365 of medial wall thickness was transient in the early phase of PAH, and the role of neointimal
366 lesions in the small PAs seemed to be greater in the progression of disease. Whereas
367 neointimal lesions are an important therapeutic target for the treatment of PAH, vascular
368 lesions with substantial fibrosis are generally considered refractory to treatment (40).
369 Therefore, we tested the anti-remodeling effect of nintedanib from 3 to 5 weeks in this study,
370 targeting non-plexiform cellular neointimal vascular lesions. The phosphorylation of PDGF
371 and FGF receptors significantly increased in the proliferative neointimal lesions and medial
372 walls in the PAH rat, indicating that these PAH-specific neointimal lesions could be a major
373 therapeutic target of nintedanib. In fact, nintedanib treatment from 3 to 5 weeks significantly
374 reduced the expression of those receptors and prevented the progression of neointimal
375 lesions, resulting in improved pulmonary hemodynamics in the PAH rats. Furthermore, we
376 showed increased expression of Twist1 protein in the lung tissue from SuHx-PAH rats.
377 Twist1 enhances the expression of TGF- β receptor and phosphorylation of SMAD2, and can
378 lead to EndMT in PA endothelial cells (41). Chronic nintedanib significantly reduced Twist1
379 protein expression in this study. These findings indicate not only the contribution of EndMT
380 in the development of proliferative occlusive neointimal lesions in PAH rats, but also the

381 anti-EndMT effects of nintedanib. Additionally, it has been reported that BIBF1000, a
382 structural precursor of nintedanib, did not disturb RV function in rats subjected to
383 mechanical pressure overload by pulmonary artery-banding (42). Another recent study also
384 showed that less dilatation, decreased fibrosis and hypertrophy of right ventricle after
385 chronic treatment with nintedanib in Su/Hx-PAH rat by echocardiography and histological
386 analysis (43), suggesting no cardiac toxicity of nintedanib.

387 A recently published study demonstrated that nintedanib had no therapeutic effect on rat
388 and human PAH (44), which contradicted our results. Several factors could explain the
389 discrepancy between the studies. For instance, rat strain that were used for experimental
390 PAH were different. A previous report has shown that the severity of the response to
391 Sugen5416 with hypoxic exposure was remarkably different between rat strains (45).
392 Actually, the RVSP of SuHx PAH in Wistar-Kyoto rats was obviously lower in a recent study
393 than in this study. Therefore, the response to nintedanib also may be dissimilar between
394 strains. As another factor, muscularization of the small PAs was evaluated to assess the
395 effect of nintedanib in a recent study. Such measurement is common for hypoxic or
396 monocrotaline-induced pulmonary hypertension models that have no neointimal lesions, but
397 it is not appropriate for the SuHx PAH rat which has neointimal lesions in the small PAs. In
398 addition, pathological images of small PAs were not shown in that study; thus, it is unclear

399 which parts of the small PAs were evaluated. Furthermore, the delivery route of nintedanib
400 to the rat was not mentioned. Thus, the possibility remain that differences in the
401 administration route of nintedanib may be the cause of the contradictory results. In contrast,
402 Huang et al. reported that chronic treatment with nintedanib reduced pulmonary vascular
403 remodeling in the Fos-related antigen-2 mouse model of systemic sclerosis (46), which was
404 supportive of our results. On the other hand, another more recent study showed that chronic
405 treatment with nintedanib of established late-phase PAH, from 8 to 11 weeks, did not
406 improved pulmonary hemodynamics and vascular remodeling in SuHx rats (43). The results
407 of these recent studies of established animal and human PAH suggest that the therapeutic
408 power of nintedanib may be limited at least in advanced stages of PAH. Although the
409 efficacy of nintedanib for mild to moderate PAH is still uncertain, the therapeutic benefit of
410 nintedanib may rest with its ability to augment the effect of other vasodilators or to prevent
411 the progression of PAH.

412 **Limitations**

413 Our study has a few limitations. First, we have not yet assessed the phenotype of
414 HPASMCs after stimulation; investigations into the effect of nintedanib on the functional
415 changes in HPASMCs may bring further beneficial information. Second, while HPASMC
416 used in this study is mainly isolated from the proximal PA, contribution of small distal PA is

417 greater than that of large proximal PA in the disease progression of PAH. Thus, data would
418 be more useful by using HPASMC isolated from only small distal PA. Third, the mechanism
419 of the inhibitory effect of nintedanib on EndMT progression is still unclear. We induced
420 EndMT in HPMVECs by using three different inducers simultaneously; nintedanib could
421 have inhibited all three signaling pathways. The inhibitory mechanism was probably very
422 complex and beyond the scope of the current study. Fourth, higher concentrations or longer
423 regimens of nintedanib treatment for PAH in the rat have not yet been evaluated. Further
424 experiments are necessary in the future to evaluate these limitations of our study.

425 **Conclusion**

426 In conclusion, we have shown the beneficial effects of nintedanib for PAH *in vitro* and *in*
427 *vivo*. Chronic treatment with nintedanib reversed the elevated pulmonary arterial pressure in
428 the PAH rat via anti-EndMT effects in HPMVECs and anti-proliferative effects in HPASMCs.
429 Moreover, an expanded indication of nintedanib for the treatment of PAH would be
430 advantageous, since nintedanib has been approved already for the treatment of other
431 human diseases with good tolerability. Although further investigations are necessary, the
432 results of this study indicate that nintedanib may be a novel additional option for the
433 treatment of human PAH, with an anti-vascular remodeling effect.

434

435 **Acknowledgments**

436 We thank Hiroshi Kawai and Reiko Mineki for their technical assistance.

437

438 **Conflict of interest:** none declared.

439

440 **Funding**

441 This work was supported by Grants-in-Aid for Scientific Research (C) from the Japan

442 Society for the Promotion of Science (25461197).

443

444 **References**

- 445 1. Lai YC, Potoka KC, Champion HC, Mora AL, Gladwin MT. Pulmonary arterial
446 hypertension: the clinical syndrome. *Circ Res*. 2014;115(1):115-30.
- 447 2. Hurdman J, Condliffe R, Elliot CA, Davies C, Hill C, Wild JM, et al. ASPIRE
448 registry: assessing the Spectrum of Pulmonary hypertension Identified at a REferral centre.
449 *Eur Respir J*. 2012;39(4):945-55.
- 450 3. Frost AE, Badesch DB, Miller DP, Benza RL, Meltzer LA, McGoon MD. Evaluation
451 of the predictive value of a clinical worsening definition using 2-year outcomes in patients
452 with pulmonary arterial hypertension: a REVEAL Registry analysis. *Chest*.
453 2013;144(5):1521-9.
- 454 4. Noskovicova N, Petrek M, Eickelberg O, Heinzelmann K. Platelet-derived growth
455 factor signaling in the lung. From lung development and disease to clinical studies. *Am J*
456 *Respir Cell Mol Biol*. 2015;52(3):263-84.
- 457 5. Perros F, Montani D, Dorfmuller P, Durand-Gasselien I, Tcherakian C, Le Pavec J,
458 et al. Platelet-derived growth factor expression and function in idiopathic pulmonary arterial
459 hypertension. *Am J Respir Crit Care Med*. 2008;178(1):81-8.
- 460 6. Benisty JI, McLaughlin VV, Landzberg MJ, Rich JD, Newburger JW, Rich S, et al.
461 Elevated basic fibroblast growth factor levels in patients with pulmonary arterial

- 462 hypertension. *Chest*. 2004;126(4):1255-61.
- 463 7. Tu L, Dewachter L, Gore B, Fadel E, Darteville P, Simonneau G, et al. Autocrine
464 fibroblast growth factor-2 signaling contributes to altered endothelial phenotype in
465 pulmonary hypertension. *Am J Respir Cell Mol Biol*. 2011;45(2):311-22.
- 466 8. Izikki M, Guignabert C, Fadel E, Humbert M, Tu L, Zadigue P, et al.
467 Endothelial-derived FGF2 contributes to the progression of pulmonary hypertension in
468 humans and rodents. *J Clin Invest*. 2009;119(3):512-23.
- 469 9. Tuder RM, Groves B, Badesch DB, Voelkel NF. Exuberant endothelial cell growth
470 and elements of inflammation are present in plexiform lesions of pulmonary hypertension.
471 *The American journal of pathology*. 1994;144(2):275-85.
- 472 10. Arciniegas E, Frid MG, Douglas IS, Stenmark KR. Perspectives on
473 endothelial-to-mesenchymal transition: potential contribution to vascular remodeling in
474 chronic pulmonary hypertension. *Am J Physiol Lung Cell Mol Physiol*. 2007;293(1):L1-8.
- 475 11. Ranchoux B, Antigny F, Rucker-Martin C, Hautefort A, Pechoux C, Bogaard HJ, et
476 al. Endothelial-to-mesenchymal transition in pulmonary hypertension. *Circulation*.
477 2015;131(11):1006-18.
- 478 12. Good RB, Gilbane AJ, Trinder SL, Denton CP, Coghlan G, Abraham DJ, et al.
479 Endothelial to Mesenchymal Transition Contributes to Endothelial Dysfunction in Pulmonary

- 480 Arterial Hypertension. *The American journal of pathology*. 2015;185(7):1850-8.
- 481 13. Suzuki T, Carrier EJ, Talati MH, Rathinasabapathy A, Chen X, Nishimura R, et al.
- 482 Isolation and characterization of endothelial-to-mesenchymal transition cells in pulmonary
- 483 arterial hypertension. *Am J Physiol Lung Cell Mol Physiol*. 2018;314(1):L118-L26.
- 484 14. Toba M, Alzoubi A, O'Neill KD, Gairhe S, Matsumoto Y, Oshima K, et al. Temporal
- 485 hemodynamic and histological progression in Sugen5416/hypoxia/normoxia-exposed
- 486 pulmonary arterial hypertensive rats. *Am J Physiol Heart Circ Physiol*.
- 487 2014;306(2):H243-50.
- 488 15. Wollin L, Wex E, Pautsch A, Schnapp G, Hostettler KE, Stowasser S, et al. Mode
- 489 of action of nintedanib in the treatment of idiopathic pulmonary fibrosis. *Eur Respir J*.
- 490 2015;45(5):1434-45.
- 491 16. Richeldi L, du Bois RM, Raghu G, Azuma A, Brown KK, Costabel U, et al. Efficacy
- 492 and safety of nintedanib in idiopathic pulmonary fibrosis. *N Engl J Med*.
- 493 2014;370(22):2071-82.
- 494 17. Nagai T, Kanasaki M, Srivastava SP, Nakamura Y, Ishigaki Y, Kitada M, et al.
- 495 N-acetyl-seryl-aspartyl-lysyl-proline inhibits diabetes-associated kidney fibrosis and
- 496 endothelial-mesenchymal transition. *Biomed Res Int*. 2014;2014:696475.
- 497 18. Zhou H, Wang Y, Zhou Q, Wu B, Wang A, Jiang W, et al. Down-Regulation of

- 498 Protein Kinase C-epsilon by Prolonged Incubation with PMA Inhibits the Proliferation of
499 Vascular Smooth Muscle Cells. *Cell Physiol Biochem*. 2016;40(1-2):379-90.
- 500 19. Muir D, Varon S, Manthorpe M. An enzyme-linked immunosorbent assay for
501 bromodeoxyuridine incorporation using fixed microcultures. *Anal Biochem*.
502 1990;185(2):377-82.
- 503 20. Wakatsuki S, Furuno A, Ohshima M, Araki T. Oxidative stress-dependent
504 phosphorylation activates ZNRF1 to induce neuronal/axonal degeneration. *J Cell Biol*.
505 2015;211(4):881-96.
- 506 21. Sakao S, Tatsumi K. The effects of antiangiogenic compound SU5416 in a rat
507 model of pulmonary arterial hypertension. *Respiration*. 2011;81(3):253-61.
- 508 22. Kuriyama S, Morio Y, Toba M, Nagaoka T, Takahashi F, Iwakami S, et al.
509 Genistein attenuates hypoxic pulmonary hypertension via enhanced nitric oxide signaling
510 and the erythropoietin system. *Am J Physiol Lung Cell Mol Physiol*.
511 2014;306(11):L996-L1005.
- 512 23. Pullamsetti SS, Berghausen EM, Dabral S, Tretyn A, Butrous E, Savai R, et al.
513 Role of Src tyrosine kinases in experimental pulmonary hypertension. *Arteriosclerosis,*
514 *thrombosis, and vascular biology*. 2012;32(6):1354-65.
- 515 24. Stenmark KR, Frid MG, Graham BB, Tudor RM. Dynamic and diverse changes in

- 516 the functional properties of vascular smooth muscle cells in pulmonary hypertension.
- 517 Cardiovasc Res. 2018;114(4):551-64.
- 518 25. Jackson AO, Zhang J, Jiang Z, Yin K. Endothelial-to-mesenchymal transition: A
519 novel therapeutic target for cardiovascular diseases. Trends Cardiovasc Med.
520 2017;27(6):383-93.
- 521 26. Li Z, Jimenez SA. Protein kinase Cdelta and c-Abl kinase are required for
522 transforming growth factor beta induction of endothelial-mesenchymal transition in vitro.
523 Arthritis Rheum. 2011;63(8):2473-83.
- 524 27. Song S, Zhang M, Yi Z, Zhang H, Shen T, Yu X, et al. The role of
525 PDGF-B/TGF-beta1/nepriylsin network in regulating endothelial-to-mesenchymal transition
526 in pulmonary artery remodeling. Cell Signal. 2016;28(10):1489-501.
- 527 28. Peng B, Lloyd P, Schran H. Clinical pharmacokinetics of imatinib. Clinical
528 pharmacokinetics. 2005;44(9):879-94.
- 529 29. Nakamura K, Akagi S, Ogawa A, Kusano KF, Matsubara H, Miura D, et al.
530 Pro-apoptotic effects of imatinib on PDGF-stimulated pulmonary artery smooth muscle cells
531 from patients with idiopathic pulmonary arterial hypertension. Int J Cardiol.
532 2012;159(2):100-6.
- 533 30. Ciucan L, Hussey MJ, Burton V, Good R, Duggan N, Beach S, et al. Imatinib

534 attenuates hypoxia-induced pulmonary arterial hypertension pathology via reduction in
535 5-hydroxytryptamine through inhibition of tryptophan hydroxylase 1 expression. *Am J Respir*
536 *Crit Care Med.* 2013;187(1):78-89.

537 31. Pankey EA, Thammasiboon S, Lasker GF, Baber S, Lasky JA, Kadowitz PJ.
538 Imatinib attenuates monocrotaline pulmonary hypertension and has potent vasodilator
539 activity in pulmonary and systemic vascular beds in the rat. *Am J Physiol Heart Circ Physiol.*
540 2013;305(9):H1288-96.

541 32. Hoeper MM, Barst RJ, Bourge RC, Feldman J, Frost AE, Galie N, et al. Imatinib
542 mesylate as add-on therapy for pulmonary arterial hypertension: results of the randomized
543 IMPRES study. *Circulation.* 2013;127(10):1128-38.

544 33. Montani D, Bergot E, Gunther S, Savale L, Bergeron A, Bourdin A, et al.
545 Pulmonary arterial hypertension in patients treated by dasatinib. *Circulation.*
546 2012;125(17):2128-37.

547 34. Guignabert C, Phan C, Seferian A, Huertas A, Tu L, Thuillet R, et al. Dasatinib
548 induces lung vascular toxicity and predisposes to pulmonary hypertension. *J Clin Invest.*
549 2016;126(9):3207-18.

550 35. Inomata M, Nishioka Y, Azuma A. Nintedanib: evidence for its therapeutic potential
551 in idiopathic pulmonary fibrosis. *Core Evid.* 2015;10:89-98.

- 552 36. Caglevic C, Grassi M, Raez L, Listi A, Giallombardo M, Bustamante E, et al.
553 Nintedanib in non-small cell lung cancer: from preclinical to approval. *Ther Adv Respir Dis*.
554 2015;9(4):164-72.
- 555 37. Rangarajan S, Kurundkar A, Kurundkar D, Bernard K, Sanders YY, Ding Q, et al.
556 Novel Mechanisms for the Antifibrotic Action of Nintedanib. *Am J Respir Cell Mol Biol*.
557 2016;54(1):51-9.
- 558 38. Voelkel NF, Gomez-Arroyo J. The role of vascular endothelial growth factor in
559 pulmonary arterial hypertension. The angiogenesis paradox. *Am J Respir Cell Mol Biol*.
560 2014;51(4):474-84.
- 561 39. Abe K, Toba M, Alzoubi A, Ito M, Fagan KA, Cool CD, et al. Formation of plexiform
562 lesions in experimental severe pulmonary arterial hypertension. *Circulation*.
563 2010;121(25):2747-54.
- 564 40. Sakao S, Tatsumi K, Voelkel NF. Reversible or irreversible remodeling in
565 pulmonary arterial hypertension. *Am J Respir Cell Mol Biol*. 2010;43(6):629-34.
- 566 41. Kwapiszewska G, Crnkovic S, Stenmark KR. A Twist on Pulmonary Vascular
567 Remodeling: Endothelial to Mesenchymal Transition? *Am J Respir Cell Mol Biol*.
568 2018;58(2):140-1.
- 569 42. de Raaf MA, Herrmann FE, Schlij I, de Man FS, Vonk-Noordegraaf A, Guignabert

570 C, et al. Tyrosine kinase inhibitor BIBF1000 does not hamper right ventricular pressure
571 adaptation in rats. *Am J Physiol Heart Circ Physiol*. 2016;311(3):H604-12.

572 43. Rol N, de Raaf MA, Sun X, Kuiper VP, da Silva Goncalves Bos D, Happe C, et al.
573 Nintedanib improves cardiac fibrosis but leaves pulmonary vascular remodeling unaltered in
574 experimental pulmonary hypertension. *Cardiovasc Res*. 2018.

575 44. Richter MJ, Ewert J, Grimminger F, Ghofrani HA, Kojonazarov B, Petrovic A, et al.
576 Nintedanib in Severe Pulmonary Arterial Hypertension. *Am J Respir Crit Care Med*. 2018.

577 45. Jiang B, Deng Y, Suen C, Taha M, Chaudhary KR, Courtman DW, et al. Marked
578 Strain-Specific Differences in the SU5416 Rat Model of Severe Pulmonary Arterial
579 Hypertension. *Am J Respir Cell Mol Biol*. 2016;54(4):461-8.

580 46. Huang J, Maier C, Zhang Y, Soare A, Dees C, Beyer C, et al. Nintedanib inhibits
581 macrophage activation and ameliorates vascular and fibrotic manifestations in the Fra2
582 mouse model of systemic sclerosis. *Ann Rheum Dis*. 2017;76(11):1941-8.

583
584

585 **Figure legends.**

586 Figure 1. Inhibitory effect of nintedanib on endothelial mesenchymal transition of human
587 pulmonary microvascular endothelial cells.

588 Inhibitory effect of nintedanib (Nin) on endothelial–mesenchymal transition (EndMT) of
589 human pulmonary microvascular endothelial cells (HPMVEC). EndMT was induced by
590 stimulation with TGF- β 2, TNF- α , and IL-1 β (Stimu). Unstimulated cells are denoted as
591 CON. Expression of (A) von Willebrand factor (vWF) and CD31 proteins, which are
592 endothelial markers, and (B) fibronectin and collagen 1 proteins, which are mesenchymal
593 markers. * $p < 0.01$ vs. CON. # $p < 0.001$ vs. Stimu. (C) Representative morphology of
594 HPMVECs in Con, Stimu, and Stimu+Nin condition.

595 .

596

597 Figure 2. Inhibitory effect of nintedanib on proliferation of human pulmonary arterial smooth
598 muscle cells.

599 (A) Inhibitory effect of nintedanib (Nin) and imatinib (Ima) on proliferation of human
600 pulmonary arterial smooth muscle cells (HPASMCs) using the CCK-8 assay. Cell viability of
601 HPASMC was assessed at 0, 12, 24, and 48 h after stimulation with multiple growth factors
602 (MGF, platelet derived growth factor-BB + fibroblast growth factor 2 + epidermal growth

603 factor + insulin-like growth factor-1). Con: control HPASMC without MGF stimulation. Values
604 are means \pm SE (n=5). * p<0.001 MGF vs. Con. § p<0.01 MGF vs. MGF + Ima. # p<0.01
605 MGF vs. MGF + Nin. ¶ p<0.05 MGF + Nin vs. MGF + Ima. (B) Inhibitory effect of Nin and
606 Ima on proliferation of HPASMC using the BrdU assay. Cell viability of HPASMC was
607 assessed at 24 and 48 h after stimulation with MGF. ** p<0.001. Plotted values are means \pm
608 SE (n=6). (C) Cell toxicity of Nin and Ima on HPASMC using the LDH assay. Values of LDH
609 were assessed at 24 and 48 h after treatment of Nin and Ima. Value of LDH in the medium
610 with Nin and Ima were normalized by that in the control medium. Plotted values are means \pm
611 SE (n=6). (D) Expressions of ERK1/2, phosphorylated ERK1/2 (pERK1/2), AKT, and
612 phosphorylated AKT (pAKT) protein with or without Nin or Ima by western blotting.
613 Representative blots are shown in the upper panels. Densitometric signals of the
614 phosphorylated protein were normalized to the corresponding non-phosphorylated protein.
615 Plotted values are means \pm SE (n=6). * p<0.01. ** p<0.001. n.s. not significantly.

616

617 Figure 3. Effect of chronic nintedanib for the development of pulmonary arterial hypertension
618 in rat.

619 (A) *In vivo* experimental timeline. Outcomes include measurement of pulmonary
620 hemodynamics and right ventricle hypertrophy, and/or morphometric analysis of pulmonary

621 arteries. Nx: control rat with normoxic condition. SuHx: single injection of Sugen 5416 with
622 chronic hypoxic exposure. W: week. (B) Chronic effect of nintedanib in Su/Hx rat.
623 Examinations of right ventricle systolic pressure (RVSP) and right ventricle weight / (left
624 ventricle and septal weight) ratio (RV/LV+S) in normoxic rats at 5 weeks [Nx(5W)], Nx rat
625 with nintedanib treatment from weeks 3 to 5 [Nx(5W) + Nin], Su/Hx rat at 3 weeks
626 [SuHx(3W)] or at 5 weeks [SuHx(5W)] after Sugen 5416 injection, and SuHx rats with
627 nintedanib treatment from weeks 3 to 5 [SuHx(5W) + Nin]. (C) Examinations of systemic
628 systolic arterial pressure (SAP), heart rate (HR), and body weight in Nx(5W), SuHx(5W),
629 and SuHx(5W) + Nin rats. Plotted values are means \pm SE (n=5). * p<0.05. ** p<0.001. ***
630 p<0.0005, **** p<0.0001.

631

632 Figure 4. Effect of chronic nintedanib for the remodeling of small pulmonary arteries.

633 (A) Representative elastic Van Gieson staining of pulmonary arteries in pulmonary
634 normotensive control rats [Nx(5W)], Sugen 5416/hypoxic rats at 5 weeks after Sugen 5416
635 injection [SuHx(5W)], and SuHx rats with nintedanib treatment from weeks 3 to 5 [SuHx(5W)
636 + Nin] (200 \times). Pulmonary arteries were divided in 50 to 200 μ m outer diameter (OD) and <
637 50 μ m OD for analysis. Scale bars indicate 50 μ m (OD 50-200) and 10 μ m (OD < 50). (B)
638 Quantitative analysis of medial wall thickness in pulmonary arteries (left; 50 to 200 μ m OD)

639 and intimal occlusive lesions in smaller pulmonary arteries (right, < 50 μm OD) in pulmonary
640 normotensive control rats at 5 weeks [Nx(5W)], Sugen 5416/hypoxic rats at 3 weeks
641 [SuHx(3W)] or at 5 weeks [SuHx(5W)] after Sugen 5416 injection, and SuHx rats with
642 nintedanib treatment from weeks 3 to 5 [SuHx(5W) + Nin]. Grade 0 (no lumen occlusion;
643 white), grade 1 (<50% occlusion; gray), grade 2 (>50% occlusion; black). Plotted values are
644 means \pm SE (n=5-6). * p<0.05. ** p<0.001. *** p<0.0001 (left). § P<0.0001 vs. Nx(5W). *
645 p<0.05 vs. SuHx(3W). # p<0.001 vs. SuHx(3W). + p<0.05 vs. SuHx(5W) (right).

646

647 Figure 5. Expression of FGF and PDGF receptors in medial and neointimal lesions of small
648 pulmonary arteries.

649 (A) Representative immunohistochemistry of phosphorylated fibroblastic growth factor
650 receptor 1 (pFGFR1) (left side) and phosphorylated platelet derived growth factor
651 receptor- β (pPDGFR- β) (right side) in pulmonary arteries (200 \times). Scale bars indicate 50
652 μm (OD 50-200) and 10 μm (OD < 50). (B) Quantitative analysis of pFGFR1 and
653 pPDGFR- β levels in pulmonary normotensive control rats at 5 weeks [Nx(5W)], Sugen
654 5416/hypoxic rats at 5 weeks [SuHx(5W)] after Sugen 5416 injection, and SuHx rats with
655 nintedanib treatment from weeks 3 to 5 [SuHx(5W)+Nin]. Pulmonary arteries were divided
656 into 50 – 200 μm outer diameter (OD) and < 50 μm OD for analysis. Plotted values are

657 means \pm SE (n=5). * p<0.0001 vs. Nx. + p<0.01 vs. Nx. # p<0.05 vs. SuHx(5W).

658

659 Figure 6. Expression of Twist1 protein in lung tissue of rats.

660 Expression of Twist1 protein by western blotting analysis in lung tissues from pulmonary

661 normotensive control rats at 5 weeks (Nx), Sugen 5416/hypoxic rats at 5 weeks [SuHx(5W)]

662 after Sugen 5416 injection, and SuHx rats with nintedanib treatment from weeks 3 to 5

663 [SuHx(5W) + Nin]. Representative blots are shown (left). Protein signals were quantified by

664 densitometric analysis, normalized to the corresponding β -actin signal, and plotted as fold

665 changes (right). The plotted values shown are means \pm SE (n=5). * p<0.001 vs. CON. #

666 p<0.05 vs. SuHx(5W).

Figure 1.

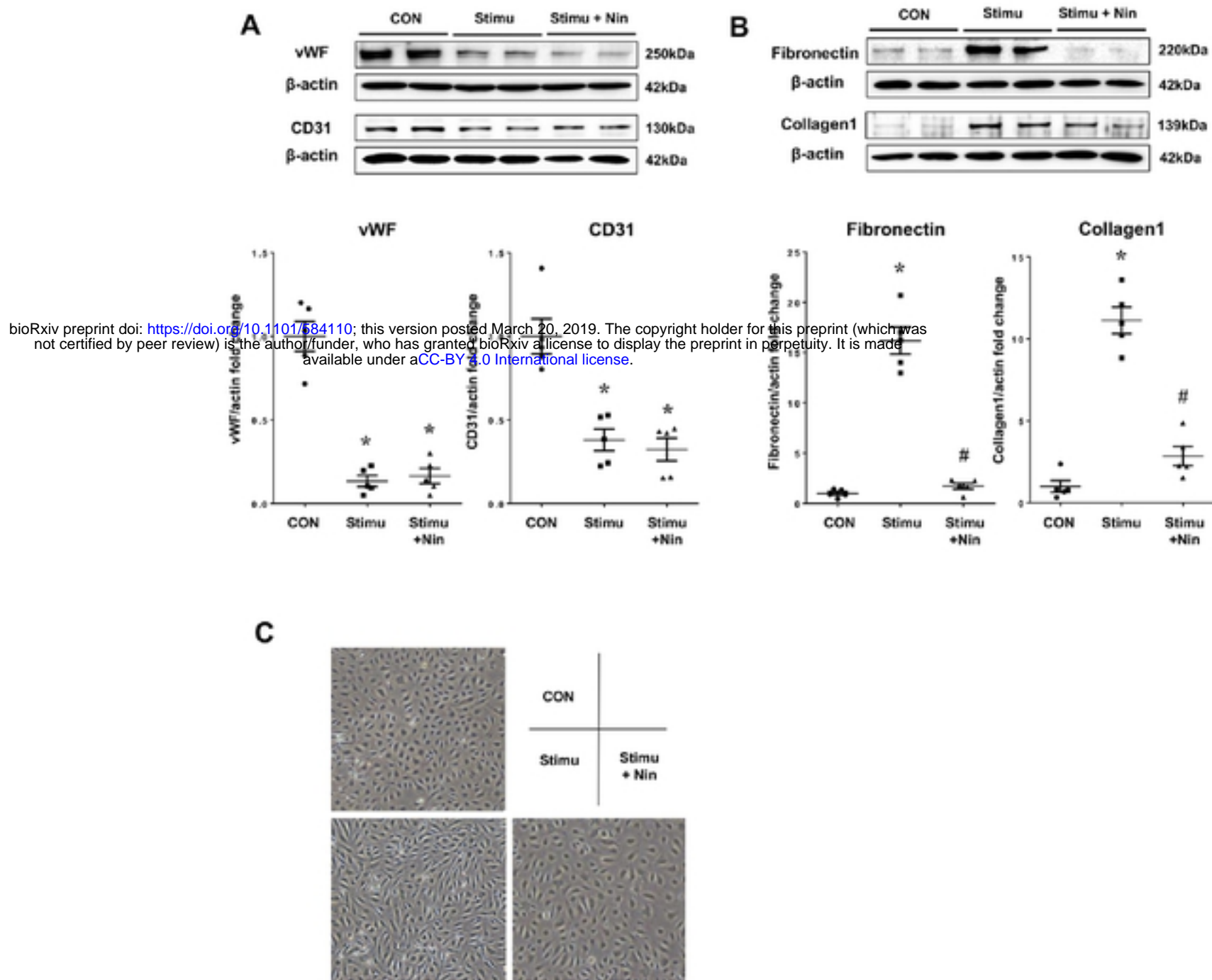


Figure 2.

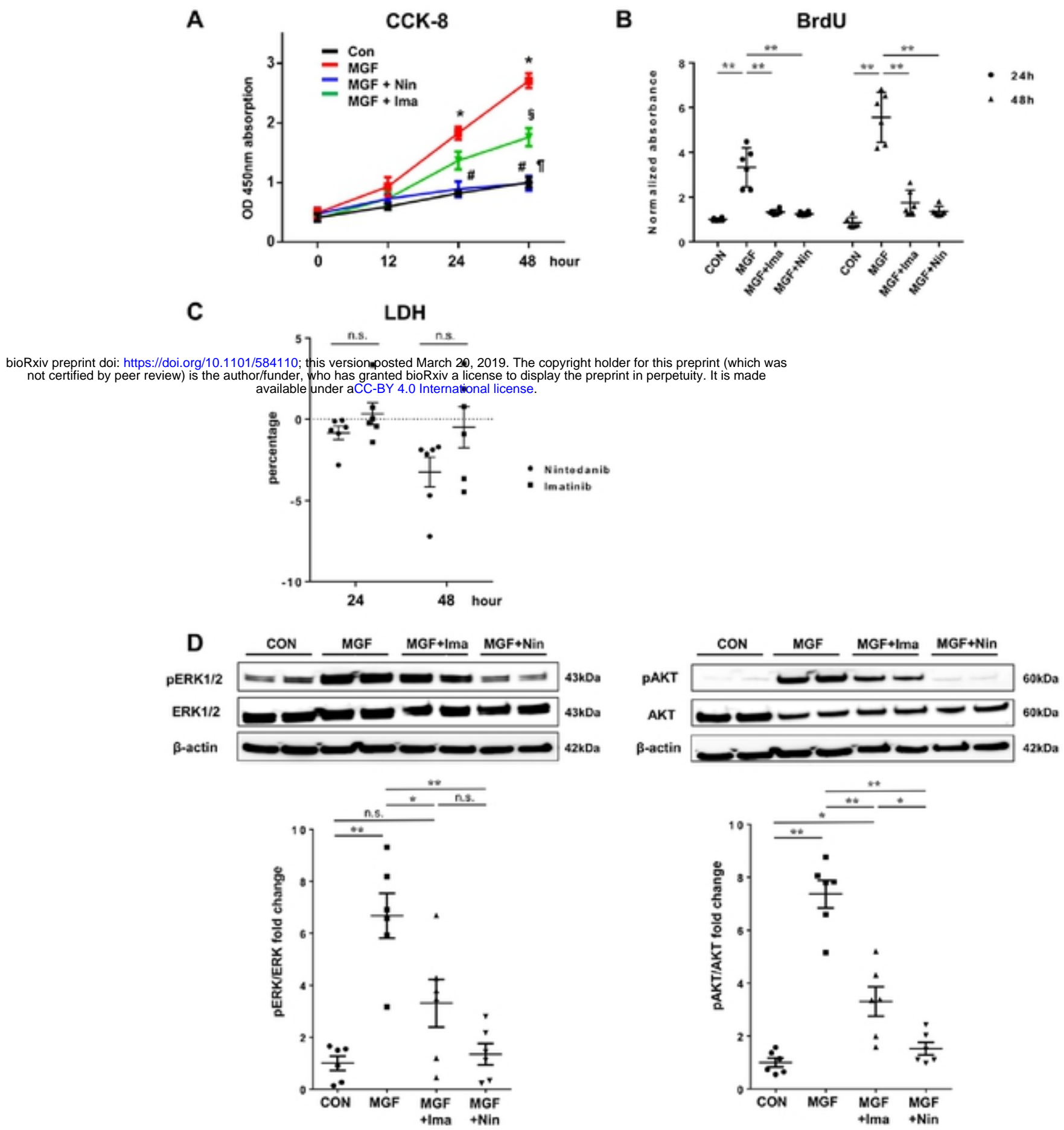
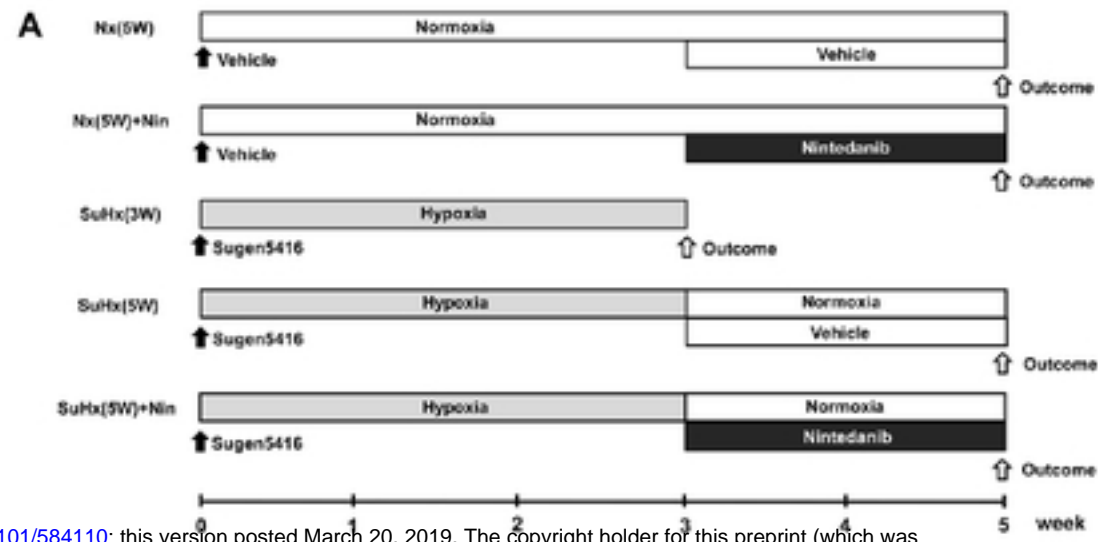


Figure 3.



bioRxiv preprint doi: <https://doi.org/10.1101/584110>; this version posted March 20, 2019. The copyright holder for this preprint (which was not certified by peer review) is the author/funder, who has granted bioRxiv a license to display the preprint in perpetuity. It is made available under aCC-BY 4.0 International license.

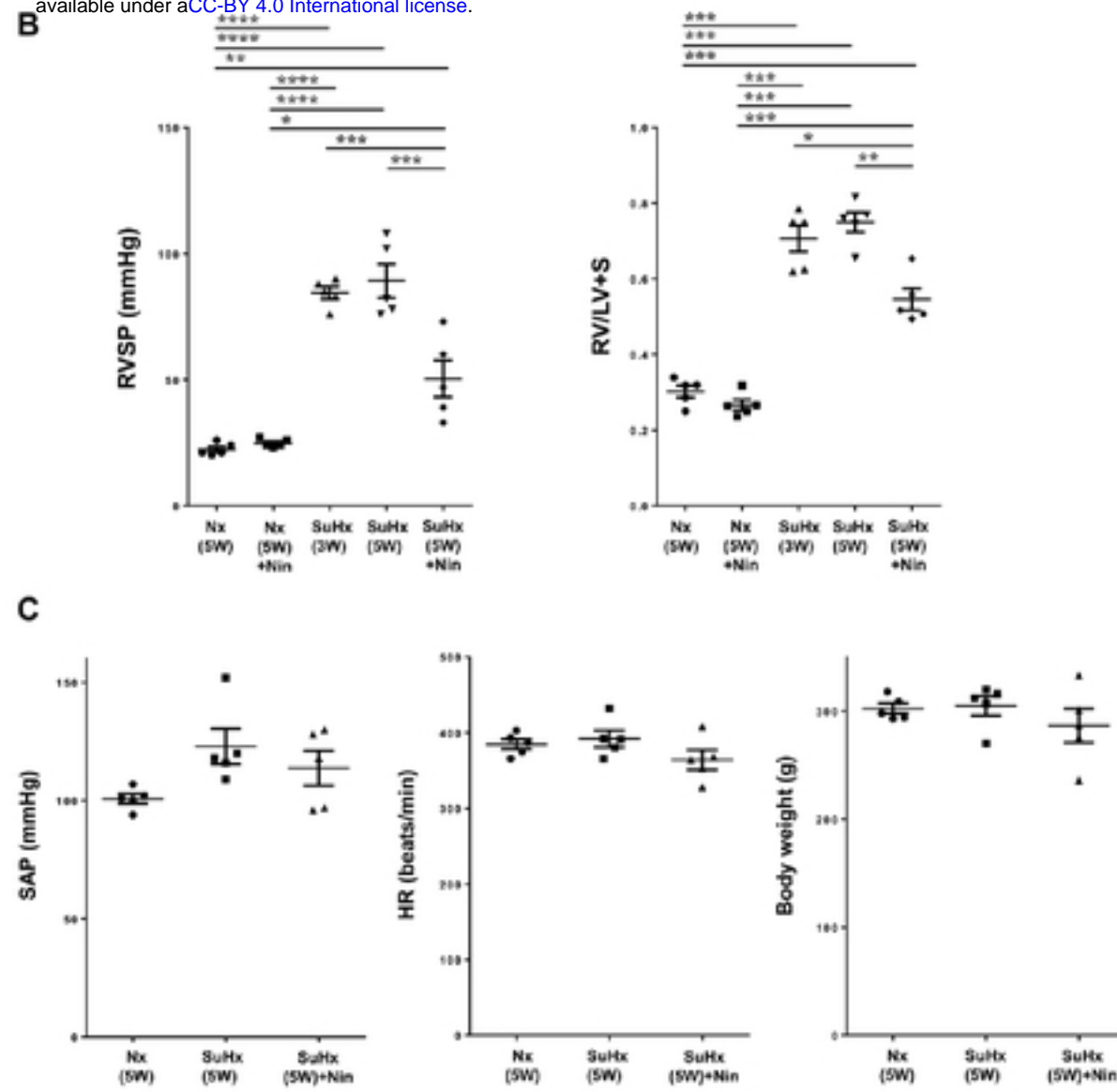
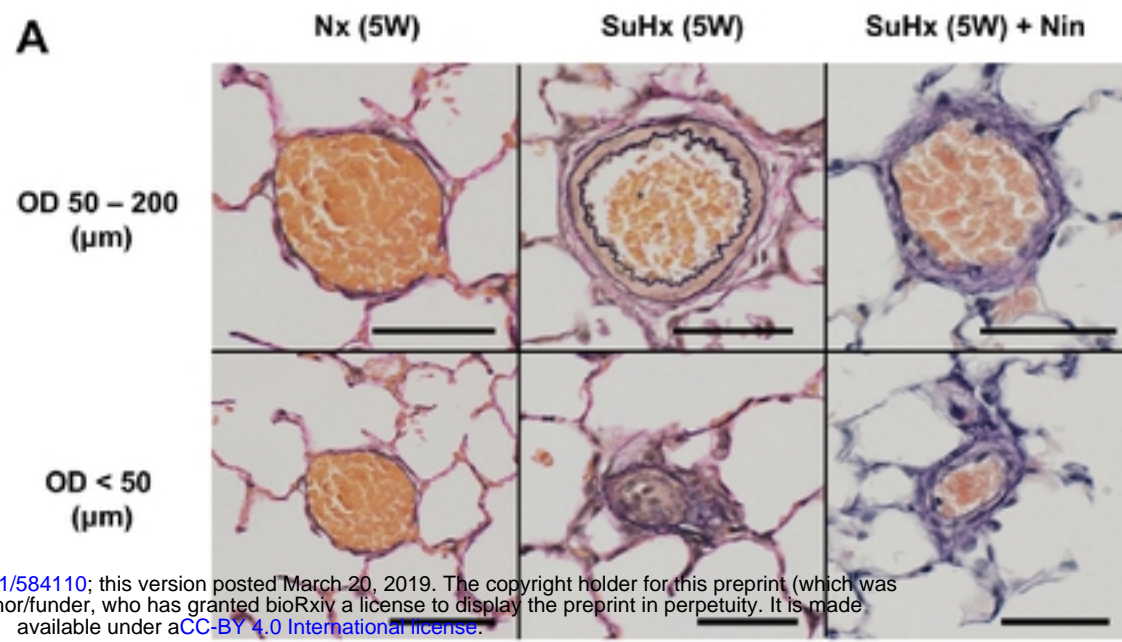


Figure 4.



bioRxiv preprint doi: <https://doi.org/10.1101/584110>; this version posted March 20, 2019. The copyright holder for this preprint (which was not certified by peer review) is the author/funder, who has granted bioRxiv a license to display the preprint in perpetuity. It is made available under aCC-BY 4.0 International license.

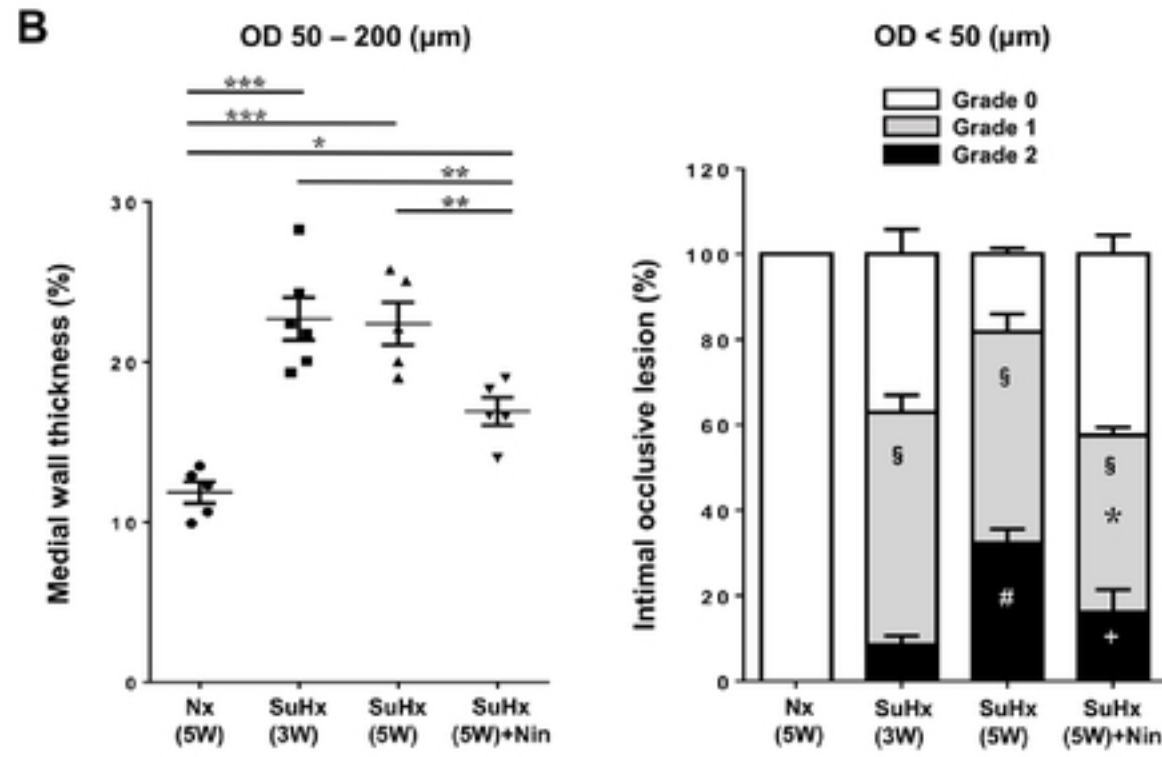


Figure 5.

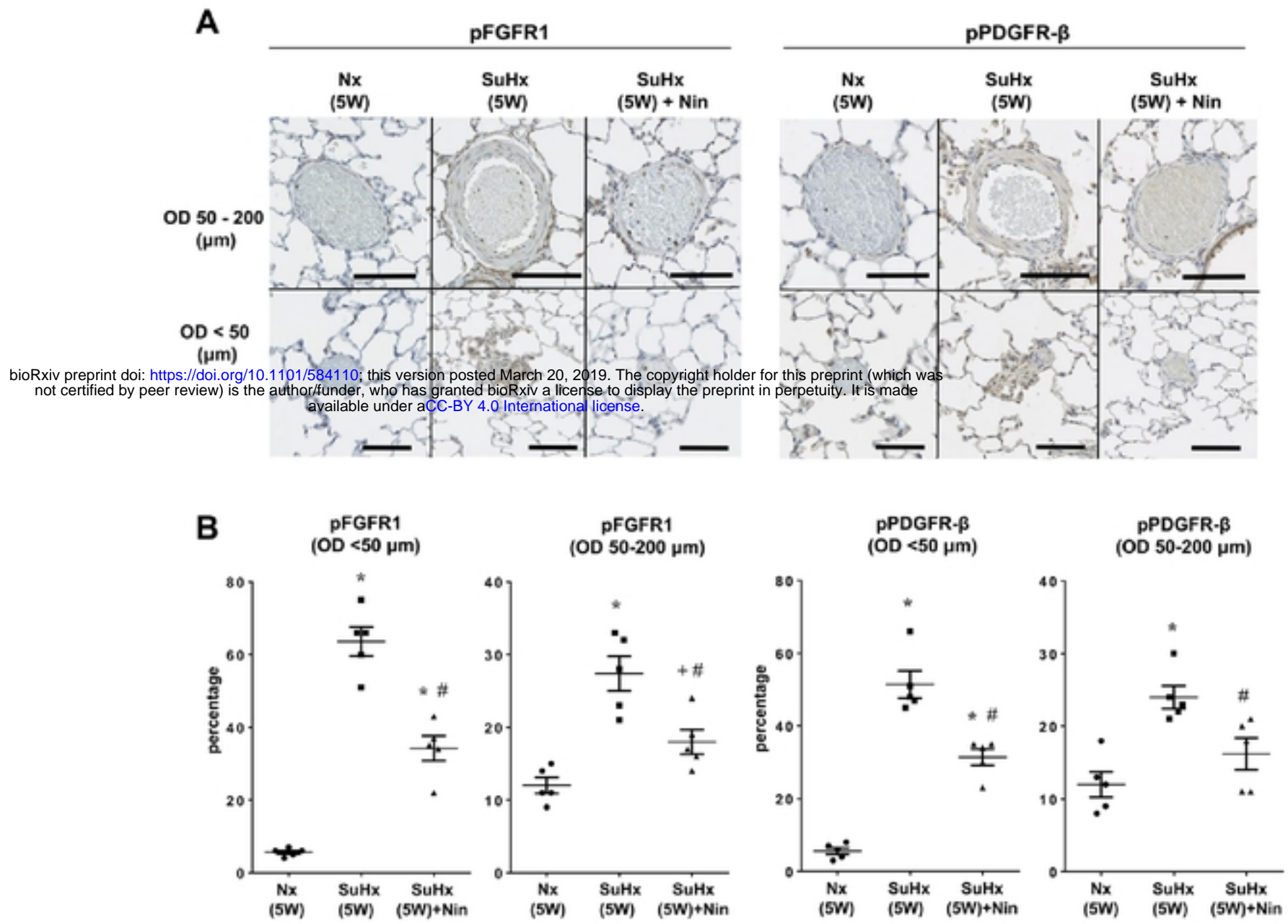
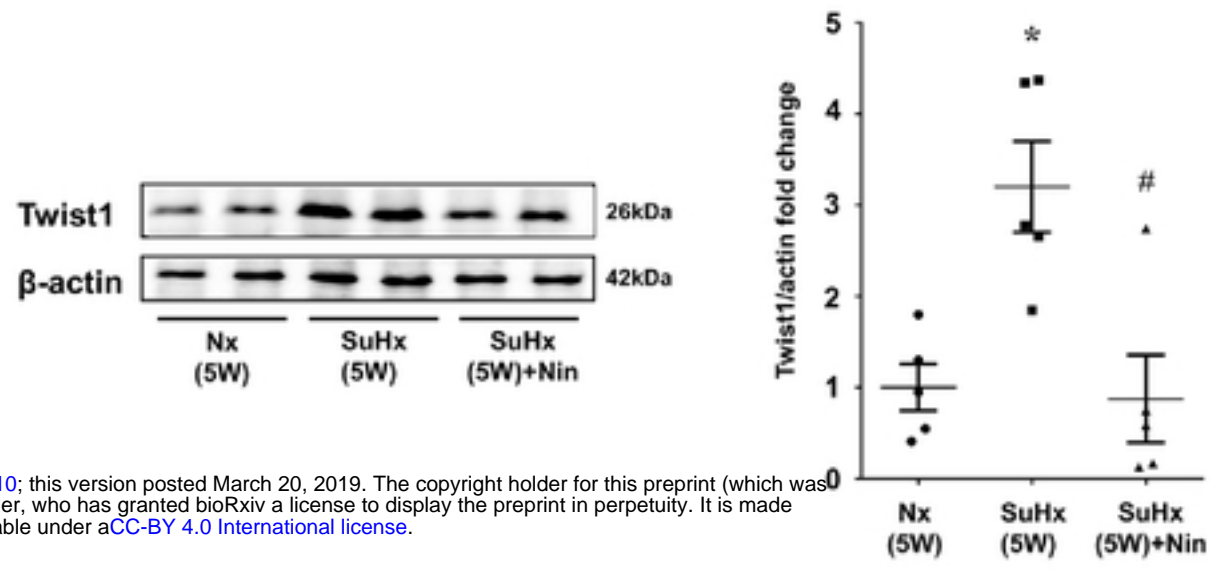


Figure 6.



bioRxiv preprint doi: <https://doi.org/10.1101/584110>; this version posted March 20, 2019. The copyright holder for this preprint (which was not certified by peer review) is the author/funder, who has granted bioRxiv a license to display the preprint in perpetuity. It is made available under aCC-BY 4.0 International license.